# Topological Data Analysis for numerical method comparisons of 2D turbulent flows

Florent Nauleau[*]
CEA, France

Thibault Bridel-Bertomeu[†]
CEA, France

Fabien Vivodtzev[‡]
CEA, France

Héloïse Beaugendre[§]
Université de Bordeaux, France

Julien Tierny[¶]
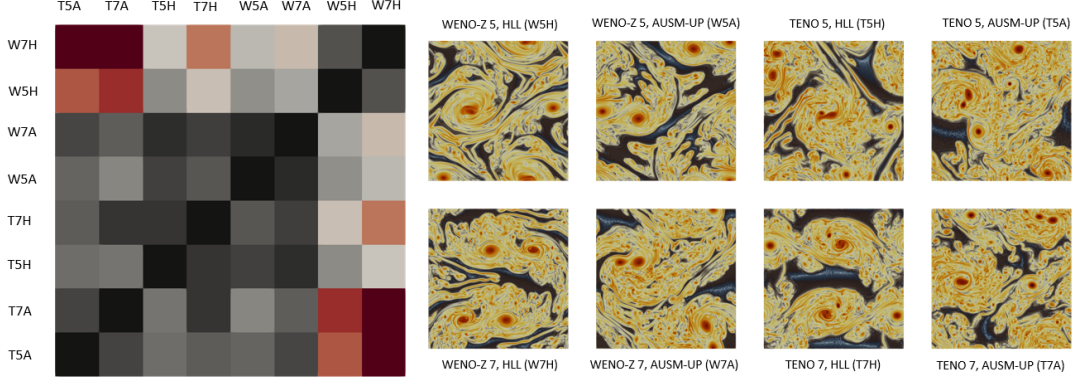CNRS, Sorbonne Université, LIP6, France

Figure 1: (left) Test cases matrix heat map and (right) developed Kelvin-Helmholtz instability at $t = 5$ obtained for the different test cases - visualization of the local enstrophy $\mathscr{E}$.

## 1 INTRODUCTION

Direct numerical simulations of two-dimensional inviscid mixing layers have been conducted to help understanding the different structures composing 2D turbulence and the interactions between the vortices over time. Because of its intrinsic multiscale nature, numerically simulating turbulence stemming from the Euler equations can be a very challenging task. Common workaround for this challenge are the increase of degrees of freedom, the use of a high-order reconstruction scheme (see *e.g.* [6, 12, 15]) and/or the use of a low-dissipation Riemann solver (see *e.g.* [18]) for finite-volume fluxes. However, there are many choices available to researchers and any of these ingredients increases the walltime of the simulation. Therefore, a thorough study of what each brings to the resolution of 2D turbulence needs to be done in order to find the best combination yielding the best resolution with the least computational time.

### 1.1 Contributions

In this ongoing work we investigate a topological data analysis approach to help the scientist choose the best combination of numerical methods to simulate turbulence. To do so, we look into the capabilities of WENO-Z [1,3,4,9] and TENO reconstruction schemes of 5th- and 7th-order [6–8] combined with different Riemann flux solvers (AUSM-up, HLL) [11, 18, 19]. Evaluating and comparing those various approaches can be very costly and it uses time not spent studying the targeted physics, *i.e.* here the behavior of 2D inviscid turbulent flows. Moreover comparing the geometrically complex shapes produced over time by a Kelvin-Helmholtz instability can be

[*]e-mail: florent.nauleau@cea.fr

[†]e-mail: thibault.bridel-bertomeu@cea.fr

[‡]e-mail: fabien.vivodtzev@cea.fr

[§]e-mail: heloise.beaugendre@math.u-bordeaux.fr

[¶]e-mail: julien.tierny@sorbonne-universite.fr

very tedious. This is why we offer in the present study a comparison procedure built on a topological abstraction of the features of the flows that eases, if not suppresses, the difficulty of comparing turbulent structures.

### 1.2 Numerical simulation of a Kelvin-Helmholtz instability

In this study, the two-dimensional compressible unsteady Euler equations for inviscid flows are solved. The system can be written as (see e.g. [13]):

$$\mathbf{U}_t + \mathbf{F}_x + \mathbf{G}_y = 0, \tag{1}$$

where the subscripts indicate differentiation, $\mathbf{U}$ is the vector of conservative dimensionless variables and $\mathbf{F}$ and $\mathbf{G}$ represent the inviscid fluxes in $x-$ and $y-$direction respectively. Those vectors are defined as follow:

$$\mathbf{U} = \begin{bmatrix} \rho \\ \rho u \\ \rho v \\ \rho E \end{bmatrix}, \quad \mathbf{F} = \begin{bmatrix} \rho u \\ \rho u^2 + p \\ \rho uv \\ (\rho E + p)u \end{bmatrix}, \quad \mathbf{G} = \begin{bmatrix} \rho v \\ \rho uv \\ \rho v^2 + p \\ (\rho E + p)v \end{bmatrix}. \tag{2}$$

In the above expressions, $t$ denotes the time and $x$ and $y$ are the Cartesian coordinates. $\rho$ denotes density, $u$ and $v$ denote the $x-$ and $y-$direction velocity components, $E$ denotes the specific total energy and $p$ denotes the static pressure. The aforementioned mathematical model is described as it is implemented in the in-house code HYPE-RION (HYPERsonic vehicle design with Immersed bOuNdaries) whose primary capabilities as a massively parallel structured solver using immersed boundary conditions have already been discussed by Bridel-Bertomeu [2]. The present study uses only regular Cartesian grids with constant grid spacings in both directions of space, $\Delta x$ and $\Delta y$, and will not rely on any immersed boundary condition during the computations presented later. This being said, the finite-volume method [10, 18, 20] is then employed for space discretization of the compressible Euler equations (1).

The 2D turbulence at the heart of this study is generated using a Kelvin-Helmholtz instability (see [14] for a complete description of
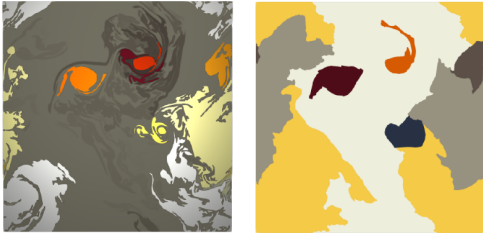
Figure 2: (left) Segmentation by merge tree and (right) segmentation by ascending Morse-Smale complex on the local enstrophy $\mathscr{E}$ of a Kelvin-Helmholtz instability at $t = 5$.
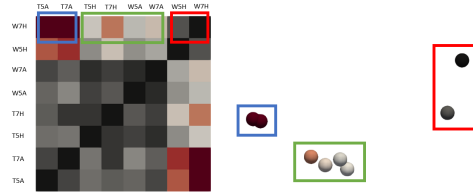


Figure 3: (left) Matrix of distances between the persistence diagrams of all numerical methods and (right) the corresponding planar view, obtained by multi-dimensional scaling.

the initialization) simulated with high-order low-dissipation WENO-Z and TENO reconstruction schemes of $5^{th}$- and $7^{th}$-order - see figure 1 for representations of the flow at $t = 5$. The numerical fluxes between the cells are obtained using either the HLL or AUSM-up Riemann solvers. To emulate turbulence in a infinite medium, all boundary conditions are set as periodic. One common measure of turbulence in two dimensions that we will rely on is the local enstrophy $\mathscr{E}$, defined locally as the square of the flow vorticity, *i.e.* $\mathscr{E} = 0.5 |\nabla \times \mathbf{u}|^2$.

## 1.3 Topological Data Analysis

Topological Data Analysis (TDA) is a recent set of techniques [16] which focus on structural features in data. Thanks to advanced concepts such as *persistent homology* [5], TDA provides tools for the multi-scale representation of the structural features of interest such as the turbulence in a flow. It also introduces distance metrics in between topological abstractions to compare such structures. In this work, we used several established techniques, readily available in the *"Topology ToolKit"* (TTK) [17].

## 2 Simulation comparison

### 2.1 TDA pipeline

We first compute the enstrophy $\mathscr{E}$ to emphasize the features of the turbulence located around vortices. Then we compute the persistence diagram for each simulation and group all diagrams. We use the persistence diagram distance matrix (according to the $L_2$-Wasserstein distance) to extract the topological distance of the enstrophy persistence between all the runs. The test cases matrix heat map can then be generated (see left part of figure 1): it gives a matrix representation from black (topologically close) to red (topologically far) of the aforementioned distances between each and every cases. To complete the pipeline we use a dimension reduction filter to clearly identify groups that are shown on figure 3.

### 2.2 Interpretation

As shown on figure 3, using a dimension reduction procedure, we could distinguish 3 groups in the matrix heat map. The blue square represents the runs done with WENO-Z of $5^{th}$- and $7^{th}$-order and the HLL solver, the green square represents the runs done with WENO-Z of $5^{th}$- and $7^{th}$-order and the AUSM-up solver and with TENO of $5^{th}$- and $7^{th}$-order and the HLL solver. The last red square groups together the runs done with the TENO of $5^{th}$- and $7^{th}$-order and the AUSM-up solver. These 3 groups we obtain using the topological analysis are consistent with the simple visual analysis of the results. Indeed, the HLL is more dissipative and leads to more difficulties in capturing the turbulence than the AUSM-up solver. What is more, the TENO schemes are by definition more fit to capture turbulence than the WENO-Z schemes [6] but they are also more computationally expensive. It is interesting to see that there are no topological differences between the results obtained with the same reconstruction schemes but at different orders - the

$7^{th}$-order schemes are more computationally expensive however. We observe on the other hand that the Riemann solver seems to be of utmost importance to capture the turbulence properly: contrary to changing the order of the reconstruction, changing the Riemann solvers had a marked impact on the end result.

## 3 Conclusion and future work

In this work, we showed that established methods from TDA could be used to compare numerical methods in CFD. Based on this comparison we are going to focus on the $5^{th}$-order TENO scheme in combination with the AUSM-up solver and further investigate the turbulence more precisely while minimizing the computation time. The ratio between a $7^{th}$-order and a $5^{th}$-order TENO scheme is indeed approximately 1.3 when it comes to computational time. This TDA pipeline is now going to be used as a preliminary setup to further investigations. Coming soon we will work with the $5^{th}$-order TENO and the AUSM-up solver to extract vortices out of the data. We will use the ascending Morse-Smale segmentation and the merge tree segmentation to try and understand the energy transfer occurring between the small and the big structures in two-dimensional turbulence - see figure 2.

## 4 Acknowledgments

## References

[1] R. Borges, M. Carmona, B. Costa, and W. S. Don. An improved weighted essentially non-oscillatory scheme for hyperbolic conservation laws. *Journal of Computational Physics*, 227(6):3191–3211, 2008.

[2] T. Bridel-Bertomeu. Immersed boundary conditions for hypersonic flows using eno-like least-square reconstruction. *Computers & Fluids*, 215:104794, 2021.

[3] M. Castro, B. Costa, and W. S. Don. High order weighted essentially non-oscillatory weno-z schemes for hyperbolic conservation laws. *Journal of Computational Physics*, 230(5):1766–1792, 2011.

[4] W.-S. Don and R. Borges. Accuracy of the weighted essentially non-oscillatory conservative finite difference schemes. *Journal of Computational Physics*, 250:347–372, 2013.

[5] H. Edelsbrunner and J. Harer. *Computational Topology: An Introduction*. AMS, 2009.

[6] L. Fu, X. Y. Hu, and N. A. Adams. A family of high-order targeted eno schemes for compressible-fluid simulations. *Journal of Computational Physics*, 305:333–359, 2016.

[7] L. Fu, X. Y. Hu, and N. A. Adams. Targeted eno schemes with tailored resolution property for hyperbolic conservation laws. *Journal of Computational Physics*, 349:97–121, 2017.

[8] L. Fu, X. Y. Hu, and N. A. Adams. A new class of adaptive high-order targeted eno schemes for hyperbolic conservation laws. *Journal of Computational Physics*, 374:724–751, 2018.

[9] F. Hu. A note on weno-z scheme. *Applied Mathematics and Computation*, 396:125886, 2021.

[10] R. J. LeVeque et al. *Finite volume methods for hyperbolic problems*, vol. 31. Cambridge university press, 2002.

[11] M.-S. Liou. A sequel to ausm, part ii: Ausm+-up for all speeds. *Journal of computational physics*, 214(1):137–170, 2006.

[12] X.-g. Liu, S. Osher, and T. Chan. Weighted essentially non-oscillatory schemes. *Journal of computational physics*, 115(1):200–212, 1994.

[13] K. Masatsuka. *I do Like CFD, vol. 1*, vol. 1. Lulu. com, 2013.

[14] O. San and K. Kara. Evaluation of riemann flux solvers for weno reconstruction schemes: Kelvin–helmholtz instability. *Computers & Fluids*, 117:24–41, 2015.

[15] C.-W. Shu and S. Osher. Efficient implementation of essentially non-oscillatory shock-capturing schemes, ii. In *Upwind and High-Resolution Schemes*, pp. 328–374. Springer, 1989.

[16] J. Tierny. *Topological Data Analysis for Scientific Visualization*. Springer, 2018.

[17] J. Tierny, G. Favelier, J. A. Levine, C. Gueunet, and M. Michaux. The Topology ToolKit. *IEEE TVCG*, 2017. `https://topology-tool-kit.github.io/`.

[18] E. F. Toro. *Riemann solvers and numerical methods for fluid dynamics: a practical introduction*. Springer Science & Business Media, 2013.

[19] E. F. Toro, M. Spruce, and W. Speares. Restoration of the contact surface in the hll-riemann solver. *Shock waves*, 4(1):25–34, 1994.

[20] J. A. Trangenstein. *Numerical Solution of Hyperbolic Partial Differential Equations*. Cambridge University Press, 2007.